Supplementary information

Nanotoxicological Evaluation of Surface Engineered WS_2 Quantum Dots in Male and Female Wistar Rats for Targeted Nucleus Imaging and Photothermal Therapy

Barkha Singh[a,b#], Rohan Bahadur[c#], Priyanka Maske[d], Dipty Singh[e*], Ajayan Vinu[c*], Rohit Srivastava[d*]

[a]Centre for Research in Nano Technology & Science (CRNTS), Indian Institute of Technology Bombay, Powai, Mumbai, India

[b] School of Biomedical Sciences and Pharmacy, The University of Newcastle, Callaghan, New South Wales, Australia

[c]Global Innovative Center for Advanced Nanomaterials (GICAN), School of Engineering, College of Engineering, Science and Environment (CESE), The University of Newcastle, Callaghan, New South Wales, Australia

[d]Department of Biosciences and Bioengineering, Indian Institute of Technology Bombay, Powai, Mumbai, India

[e]Department of Neuroendocrinology, National Institute for Research in Reproductive and Child Health (NIRRCH), Parel, Mumbai, India

***Corresponding authors**

Dr. Dipty Singh[e*]

*E-mail: singhd@nirrch.res.in

[e] Department of Neuroendocrinology, National Institute for Research in Reproductive and Child Health (NIRRCH), Parel, Mumbai, 400012, India

Dr. Ajayan Vinu[c]*

*E-mail: ajayan.vinu@newcastle.edu.au

[c] Global Innovative Center for Advanced Nanomaterials (GICAN), School of Engineering, College of Engineering, Science and Environment (CESE), The University of Newcastle, Callaghan, New South Wales 2308, Australia

Dr. Rohit Srivastava[d*]

*E-mail: rsrivasta@iitb.ac.in

[d] Department of Biosciences and Bioengineering, Indian Institute of Technology Bombay, Powai, Mumbai, 400076, India

 # equal contribution

Table of Contents

Material and Method

1. Cell Culture

1.1. Biocompatibility

1.2. THP-1 cells differentiated macrophage-like cells

1.3. ROS generation

1.4 Hemolysis assay

1.5 Confocal microscopy for bio-imaging of cells

1.6 Photothermal transduction

1.7 *In-vitro* photothermal cytotoxicity and Effect of QDs mediated PTT on cancer cells cycle

List of Figures

Figure S1: TEM image of WS_2 QDs synthesized with 0.1:1 PEG:WS_2.

Figure S2: (a) SEM image, and **(b,c)** TEM image **(b inset:** SAED pattern**)** for PEG_WS_2 QDs

Figure S3: TEM image of WS_2 QDs considered as control

Figure S4: Wide angle XPS spectrum for PEG_WS_2 QDs

Figure S5*:* FTIR spectroscopy of PEG_WS_2 QDs, **(b)** Contact angle for WS_2 QDs without PEG modification

Figure S6: pH dependent **a)** UV-Vis abosrbance spectra, **b)** photoluminescence spectra under an excitation wavelength of 300 nm, **c)** long term photoluminescence spectrum at an excitation wavelength of 300 nm for PEG_WS_2 QDs

Figure S7: Characterization of PVP_WS_2 QDs, **(a)** UV-Vis absorbance spectrum, **(b)** digital image under UV light depicting the photoluminescence for the material, **(c)** photoluminescence spectra under an excitation wavelength of 300 nm, **(d-f)** TEM images for the materials at different magnifications.

Figure S8: Characterization of PEI_WS_2 QDs, **(a)** UV-Vis absorbance spectrum (**inset:** digital image under normal light), **(b)** photoluminescence spectra under an excitation wavelength of 300 and 350 nm (**inset:** digital image under UV light depicting the photoluminescence for the material), **(c-d)** TEM images for the materials at different magnifications.

Figure S9: Morphology of Breast cancer cells MDAMB **(a-b)** Untreated cells **(c-d)** cells treated with laser only **(e-f)** Cells treated with PTT using 100 ppm of PEG_WS_2 QDs **(g-h)** Cells treated with PTT using 200 ppm of PEG_WS_2 QDs

Figure S10: Biodistribution of PEG_WS_2 QDs in different organs of (a) male and (b) female rats on day 14.

Material and Method:

1. Cell culture:

1.1. **Biocompatibility:** Mouse fibroblast cell line L929 and breast cancer cell line MDA-MB-231 were cultured in Dulbecco's Modified Eagle Medium (DMEM) supplemented with 10% fetal bovine serum and 1% antibiotic solution. Cells were sub-cultured at 75% confluence. Cells were trypsinized and 6000 cells per well were seeded in a 96 well plate. The cells (n=6) were allowed to adhere before varying concentrations of material (25-1000 µg mL^{-1}) were added and then cultured for 24 hours. After washing the cells with PBS, Resazurin dye was added to each well. The dye was incubated for 4 hours following which reading was taken in a plate reader. Untreated cells served as the negative control, whereas Triton-X 100-treated cells served as the positive control (PC). Statistical significance was assessed using an unpaired two-tailed Welch's t-test (ns, not significant; * $p < 0.05$; ** $p < 0.01$; *** $p < 0.001$).

1.2. **THP-1 cells differentiated macrophage-like cells:** The THP-1 cells were grown in RPMI-1640 media and were sub-cultured at a density of $8x10^5$ cells/mL. They were then seeded into a 96-well plate. The THP-1 cells were differentiated into macrophages by treating them with 25 ng/mL of phorbol 12-myristate-13-acetate (PMA) for 24 hours. Afterwards, the differentiated macrophages were washed with PBS and fresh media was added. The cells were then kept in the incubator for an additional 24 hours. Afterwards, various concentrations of nanomaterials (25-1000 µg/mL) were added to the macrophages and incubated for 24 hours. The cells were then washed with PBS and resazurin dye was added. The intensity of absorbance and fluorescence was measured using a plate reader after 4 hours of incubation. Statistical significance was assessed using an unpaired two-tailed t-test (ns, not significant;* $p < 0.05$; ** $p < 0.01$; *** $p < 0.001$).

1.3. **ROS generation:** L929 cells were seeded at a density of $6x10^3$ cells per well in a 96-well plate and incubated overnight at 37 °C in a 5% CO_2 incubator. The cells were treated with different concentrations of the QDs for 24 hours. DCFDA dye was added to the cells at a final concentration of 5 µM, and the plate was incubated for an additional 30 minutes at 37°C. The plate was then read on a plate reader at an excitation wavelength of 485 nm and an emission wavelength of 538 nm to measure the fluorescence intensity, which is directly proportional to the level of ROS generated in the cells. Cells treated with H_2O_2 were taken as positive control while untreated cells were considered as NC. The experiment was conducted in triplicate and the results were plotted average±standard deviation. Unpaired T-test was performed to

determine the significance of the effect of the QDs on the generation of ROS compared to control cells (ns, not significant;* $p < 0.05$, ** $p < 0.01$, *** $p < 0.001$).

1.4. **Hemolysis assay:** The compatibility of QDs with blood was evaluated using blood samples obtained from healthy participants, with the approval and clearance from the Institutional Ethics Committee (No. IITB-IEC/2019/031) at IIT Bombay. The collected whole blood was diluted with PBS and centrifuged for 5 minutes at 1000 rpm. The resulting pellet was resuspended in PBS, and multiple centrifugations and redispersion cycles were performed until the supernatant was clear and only red blood cells (RBCs) remained. QDs in various concentrations (100-2000 µg/mL) were added to an equal volume of isolated RBCs (200 µL). Triton X-100 treated RBCs were used as a positive control, while RBCs treated with PBS were used as a negative control. All the samples were centrifuged for 5 minutes at 4000 rpm after 2 hours of incubation at 37 °C. Digital images of the pellet were taken, and the supernatant was carefully withdrawn into a 96-well plate, and its absorbance was measured at 540 nm using a plate reader. PBS was used as a blank. The percentage of hemolysis was calculated using the following equation:

Hemolysis (%) = [(Intensity of sample - Intensity of media blank) / (Intensity of positive control - Intensity of media blank)] x 100

The morphology of the red blood cells (RBCs) was observed using environmental scanning electron microscopy (ESEM). The RBCs were fixed using 2% glutaraldehyde overnight at 4°C. After that, they were washed with PBS and drop-casted onto an aluminum foil. The sample was then examined under the ESEM. Statistical significance was assessed using an unpaired two-tailed Welch's t-test (ns, not significant;*$p < 0.05$; **$p < 0.01$; ***$p < 0.001$)

1.5. **Confocal microscopy for bio-imaging of cells:** Cells were cultured as mentioned above. 25 μgmL^{-1} PEG_WS_2 QDs were incubated with L929/MDAMB cells for 24 hours. Cells were then washed with PBS and fixed using 4% formaldehyde. The cells were then observed using DAPI filter under laser scanning confocal microscope. L929 Control cells were incubated with DAPI for comparison.

1.6. **Photothermal transduction:** Different concentration of PEG_WS_2 QDs was irradiated with 808 nm laser ($1W/cm^2$) up to 10 minutes in a 96 well plate and the rise in temperature was recorded using temperature probe.

1.7. ***In-vitro*** **photothermal cytotoxicity and Effect of QDs mediated PTT on cancer cells cycle:** To evaluate the in-vitro photothermal cytotoxicity of PEG_WS_2 QDs nanoparticles, MDAMB-231 cells were seeded onto a 96-well plate and allowed to attach. The cells were washed, and nanomaterials containing 50, 100, and 200 ppm of PEG_WS_2 QDs were added. After 24 hours of incubation, laser irradiation was conducted for 5 minutes using an 808 nm laser system. The cells were then kept in an incubator overnight, following which an alamar assay was performed.

To study the effects of PEG_WS_2 QDs mediated PTT on cell cycle of MDAMB, the cells were seeded in a 6-well plate and allowed to incubate overnight. Fresh media containing the QDs was then added to the cultured medium, and the cells were incubated for 24 hours. After this incubation period, the cells were washed with PBS twice, trypsinized, and irradiated with an 808 nm NIR laser for 10 minutes. The cells were then transferred back to a 6-well plate and allowed to attach overnight. Following this, the cells were washed with PBS, harvested using trypsin, and centrifuged. The resulting pellet was fixed using chilled 70% ethanol dropwise and left to fix for 30 minutes at 4°C. The cells were then centrifuged again, resuspended, and incubated with RNAse (50 µL of 100µg mL^{-1}) and propidium iodide (200µl from 50µg mL^{-1}). The cell populations in G1, S, and G2 were then analyzed using FlowJo software after flow cytometry analysis.

Table S1: Table comparing different theranostic probes in literature and their photothermal properties.

Material	Laser Power ($W\ cm^{-2}$)	Laser (nm)	Concentration ($mg\ mL^{-1}$)	PTT transduction (Δ °C) / Time (mins)	Ref.
GQD	0.9	808	1.7	10 / 10	[1]
BPQDs	1	808	0.2	31.5 / 10	[2]
GeQDs	2	808	0.2	55.5 / 5	[3]
AMQDs	2	808	0.1	50 / 5	[4]
GM/OD/Mn_3O_4 hydrogel	1	808	0.25	8 / 4.5	[5]
Fe_3O_4 NPs	1	808	0.2	22.5 / 10	[6]
TiN@$mSiO_2$-Fe_3O_4/PEI	1	808	0.2	35.1/10	[7]
MoS_2 NSs	0.47	785	0.03	27.5 / 5	[8]
18.75% CQDs/MoS2	1.5	808	0.1	34.8 / 10	[9]
PEG_WS_2 QDs	1	808	0.25	23 / 2	**This work**

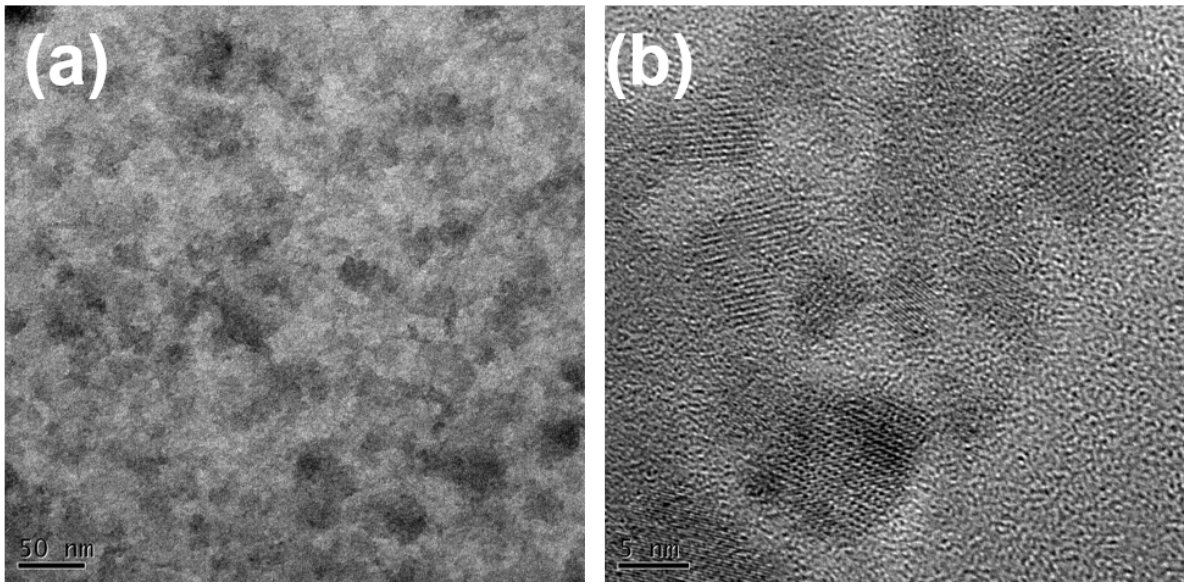

Figure S1: TEM image of WS_2 QDs synthesized with 0.1:1 PEG:WS_2.

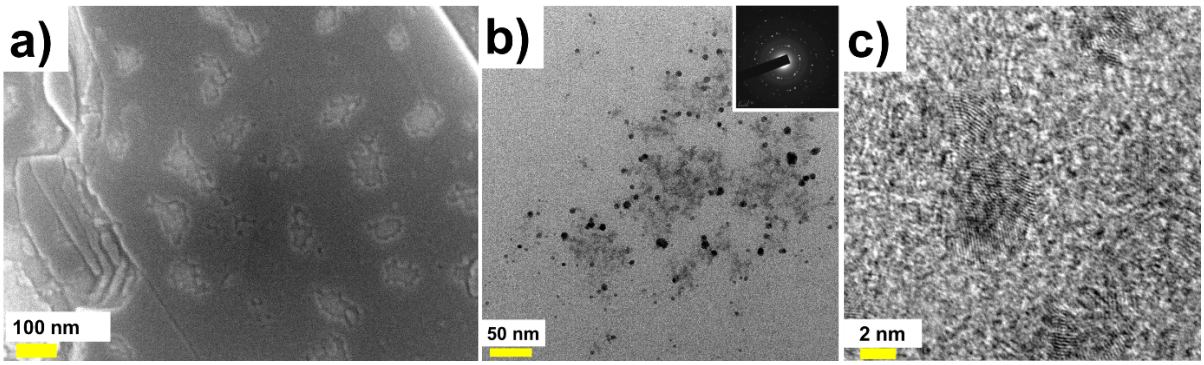

Figure S2: (a) SEM image, and **(b,c)** TEM image **(b inset:** SAED pattern**)** for PEG_WS_2 QDs

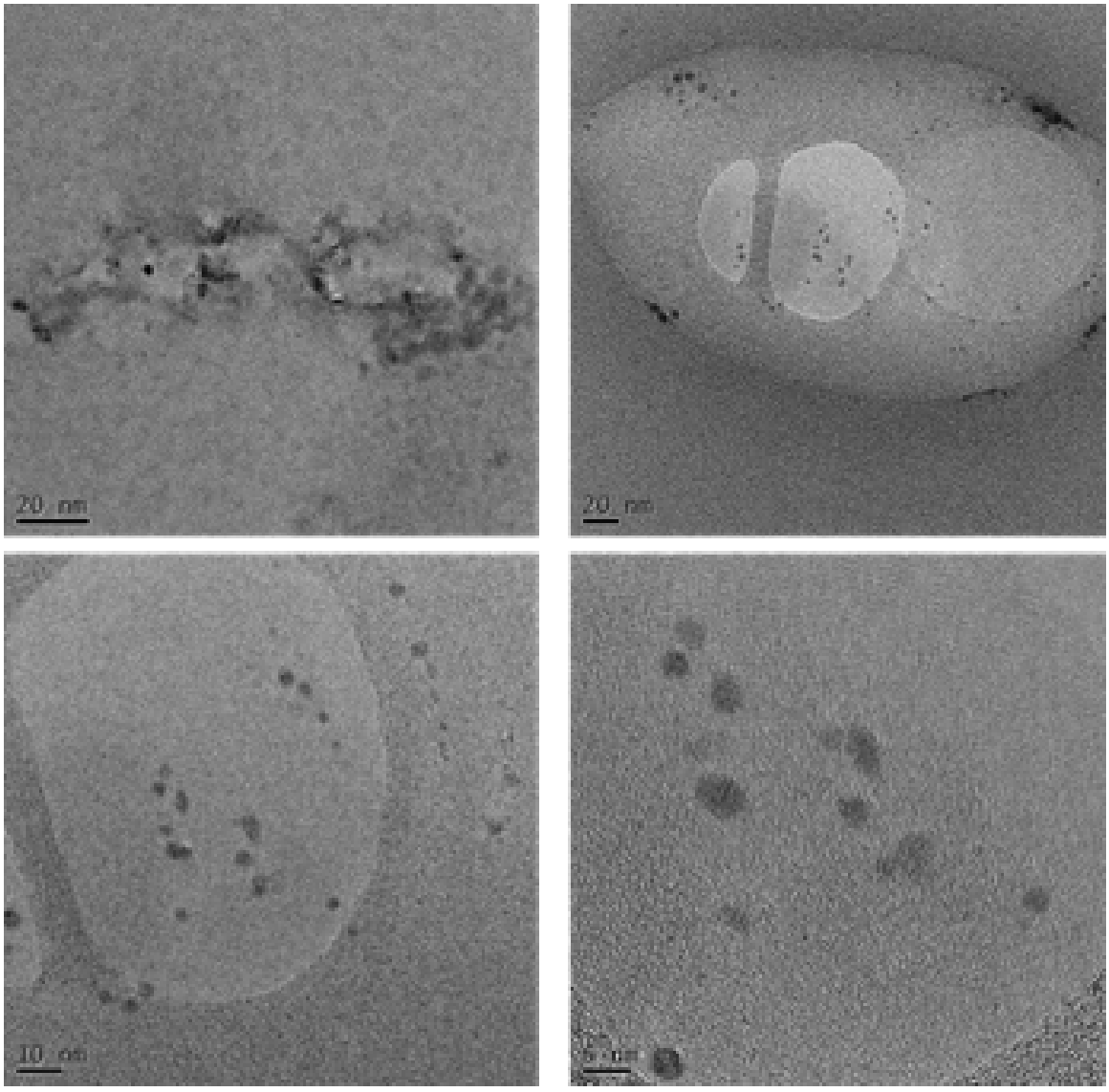

Figure S3: TEM image of WS_2 QDs considered as control

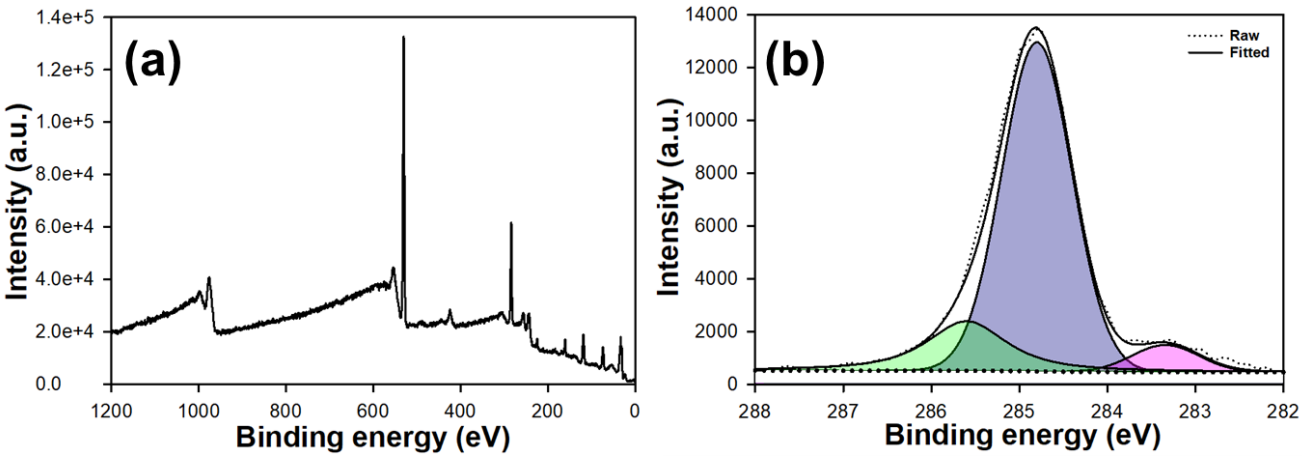

Figure S4: (a) Wide angle and **(b)** C1s high resolution XPS spectrum for PEG_WS_2 QDs

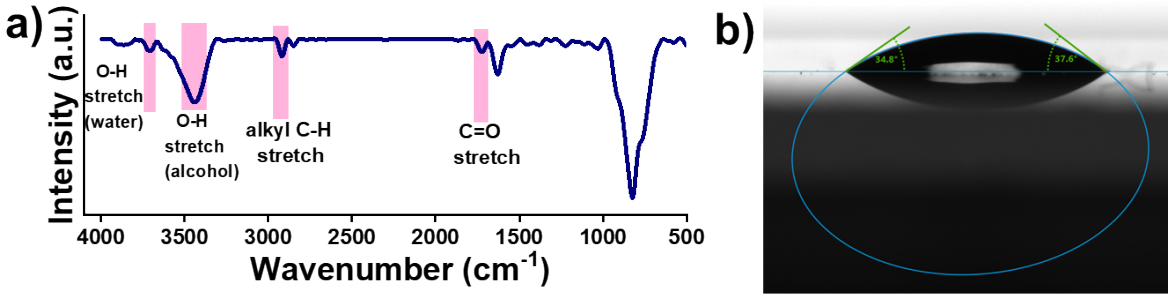

Figure S5: (a) FTIR spectroscopy of PEG_WS_2 QDs, **(b)** Contact angle for WS_2 QDs without PEG modification

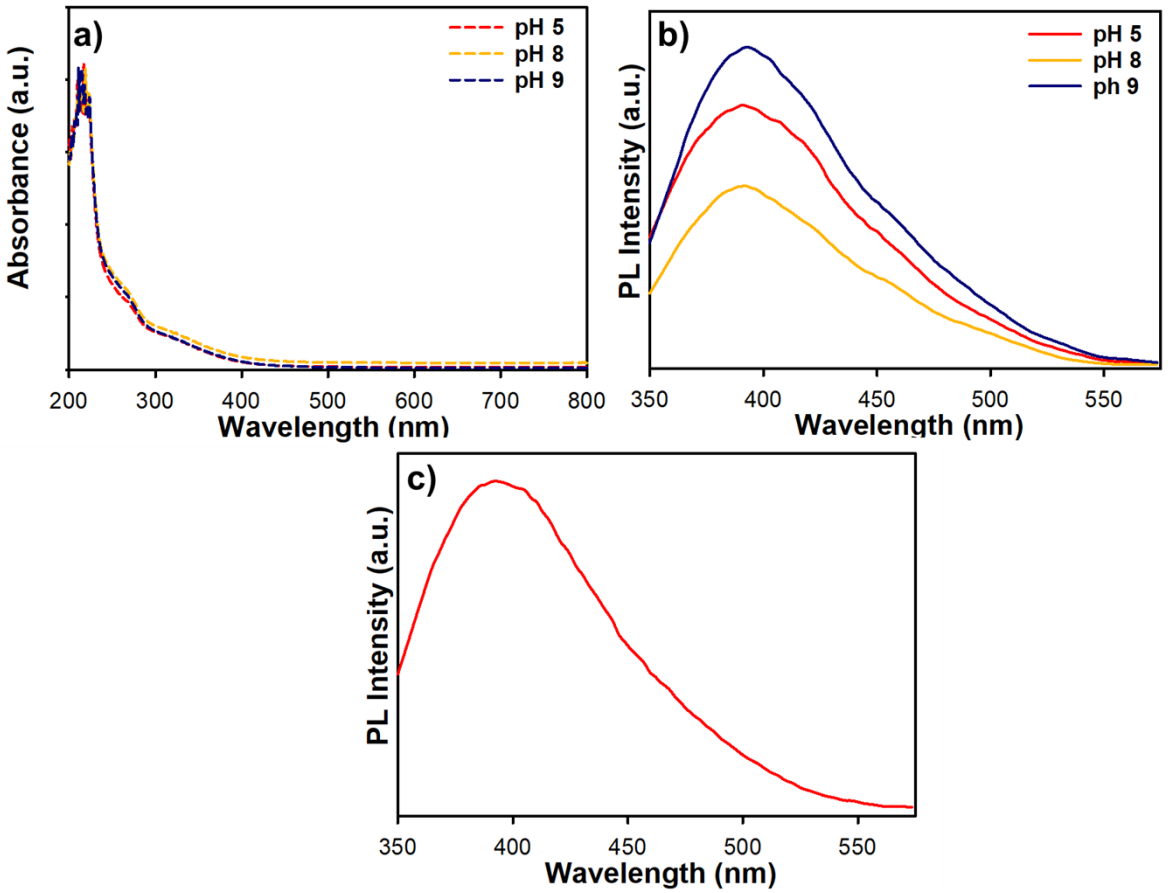

Figure S6: pH dependent **a)** UV-Vis abosrbance spectra, **b)** photoluminescence spectra under an excitation wavelength of 300 nm, **c)** long term photoluminescence spectrum at an excitation wavelength of 300 nm for PEG_WS_2 QDs

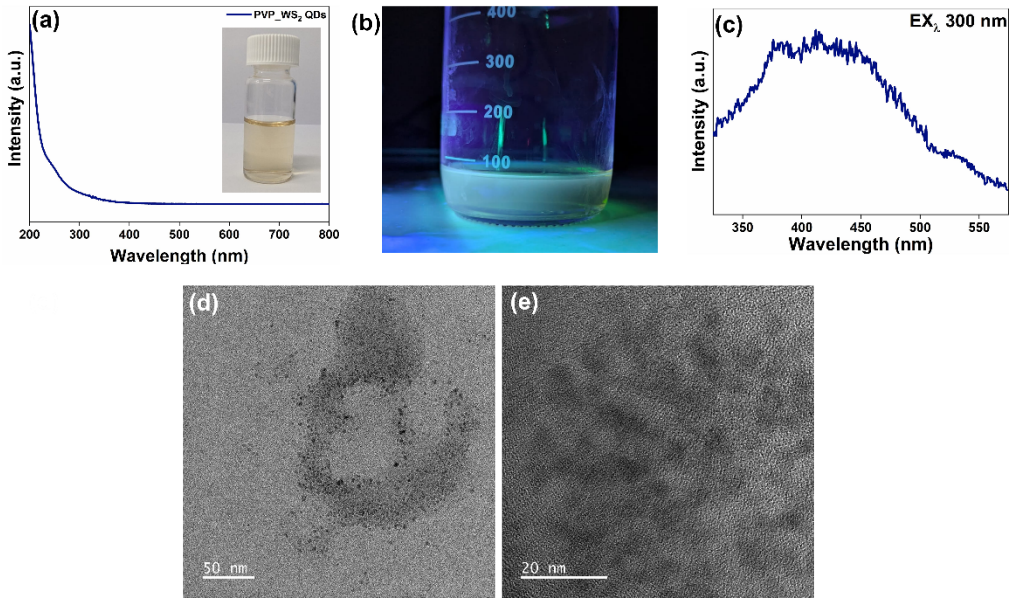

Figure S7: Characterization of PVP_WS_2 QDs, **(a)** UV-Vis absorbance spectrum, **(b)** digital image under UV light depicting the photoluminescence for the material, **(c)** photoluminescence spectra under an excitation wavelength of 300 nm, **(d,e)** TEM images for the materials at different magnifications.

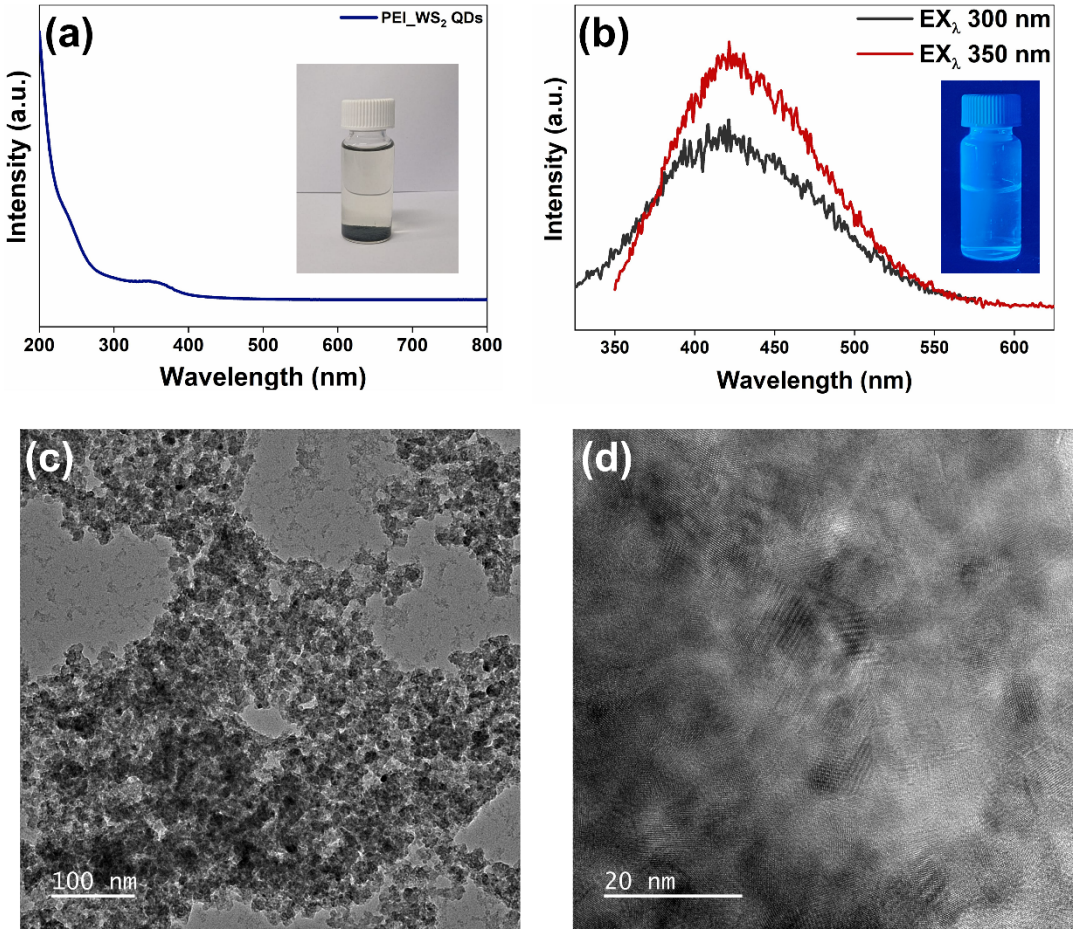

Figure S8: Characterization of PEI_WS_2 QDs, **(a)** UV-vis absorbance spectrum (**inset:** digital image under normal light), **(b)** photoluminescence spectra under an excitation wavelength of 300 and 350 nm (**inset:** digital image under UV light depicting the photoluminescence for the material), **(c-d)** TEM images for the materials at different magnifications

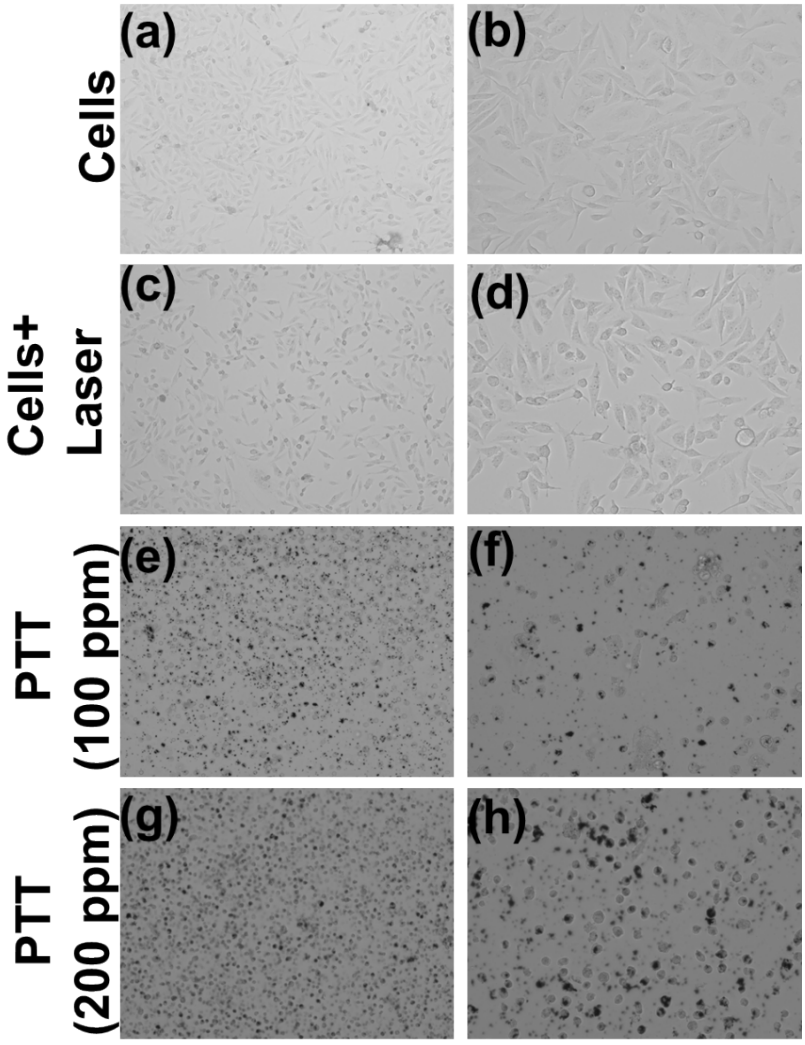

Figure S9: Morphology of Breast cancer cells MDAMB **(a-b)** Untreated cells **(c-d)** cells treated with laser only **(e-f)** Cells treated with PTT using 100 ppm of PEG_WS_2 QDs **(g-h)** Cells treated with PTT using 200 ppm of PEG_WS_2 QDs

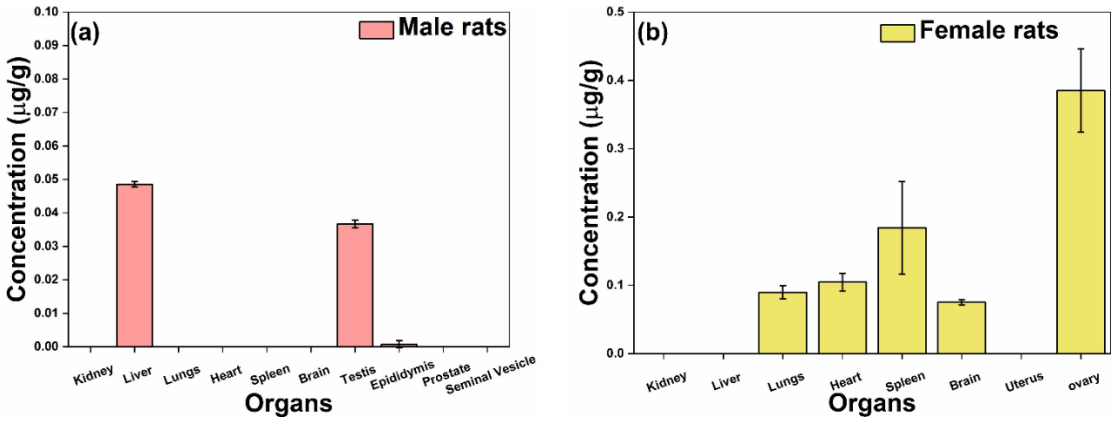

Figure S10: Biodistribution of PEG_WS_2 QDs in different organs of **(a)** male and **(b)** female rats on day 14.

References:

1. Bong Lee, Gretel A. Stokes, Alina Valimukhametova, Steven Nguyen, Roberto Gonzalez-Rodriguez, Adam Bhaloo, Jeffery Coffer, Anton V. Naumov, Automated Approach to In Vitro Image-Guided Photothermal Therapy with Top-Down and Bottom-Up-Synthesized Graphene Quantum Dots, *Nanomaterials*, **2023**, 13, 805.

2. Dr. Zhengbo Sun, Hanhan Xie, Siying Tang, Prof. Xue-Feng Yu, Zhinan Guo, Jundong Shao, Prof. Han Zhang, Hao Huang, Prof. Huaiyu Wang, Prof. Paul K. Chu, Ultrasmall Black Phosphorus Quantum Dots: Synthesis and Use as Photothermal Agents, *Angewandte Chemie*, **2015**, 54, 39, 11526-11530.

3. Jiang Ouyang, Chan Feng, Dr. Xiaoyuan Ji, Dr. Li Li, Hemanth Kiran Gutti, Na Yoon Kim, Dolev Artzi, Angel Xie, Dr. Na Kong, Prof. You-Nian Liu, Prof. Guillermo J. Tearney, Prof. Xinbing Sui, Dr. Wei Tao, Prof. Omid C. Farokhzad, 2D Monoelemental Germanene Quantum Dots: Synthesis as Robust Photothermal Agents for Photonic Cancer Nanomedicine, *Angewandte Chemie*, **2019**, 58, 38, 13405-13410.

4. Wei Tao, Xiaoyuan Ji, Dr. Xiaoding Xu, Dr. Mohammad Ariful Islam, Zhongjun Li, Si Chen, Dr. Phei Er Saw, Prof. Han Zhang, Zameer Bharwani, Zilei Guo, Prof. Jinjun Shi, Prof. Omid C. Farokhzad, Antimonene Quantum Dots: Synthesis and Application as Near-Infrared Photothermal Agents for Effective Cancer Therapy, *Angewandte Chemie*, **2017**, 129, 39, 12058-12062.

5. Yao Zhao, Wenkai Wang, Mingyi Liu, Yunfan Cai, Yan Wang, Yan Dong, Yong-kang Bai, Juanfang Zhu, Franklin R. Tay, Lina Niu, Mn_3O_4-potentiated bifunctional hydrogel for mild temperature-controlled tumor ablation and osteogenesis, *Bioactive Materials*, **2026**, 55, 391-409

6. Xuan Shang, Mingyue He, Huiying Jiang, Fangying Jiang, Deping Wang, Jimin Cao, Yan Tan, Jigen Li, Yanlin Feng, Xin Zhou, Porous Fe_3O_4-GOx Theranostic Nanoplatform for Tumor Imaging and Starvation/Photothermal Synergistic Therapy, *Colloids and Surfaces B: Biointerfaces*, **2026**, 262, 115526

7. Ruiqi Yang, Zhu You, Bojun Xie, Mingyang Liu, Eva Yazmin Santiago, Lucas V. Besteiro, Yong Wang, Baojin Ma, Hong Liu, Dongling Ma, Plasmon-boosted titanium nitride-based nanoplatform for synergistic photothermal-chemodynamic cancer therapy with smart degradability, *Biomaterials*, **2026,** 123950

8. Yuqian Zhang, Weijun Xiu, Yiting Sun, Di Zhu, Qi Zhang, Lihui Yuwen, Lixing Weng, Zhaogang Teng, Lianhui Wang, RGD-QD-MoS_2 nanosheets for targeted fluorescent imaging and photothermal therapy of cancer, *Nanoscale* **2017**, 41, 9, 15835-15845

9. Yayu Chen, Pengcheng Huang, Wenting Hong, Wanqing Xu, Xiaoping Chen, Shuxian Li, Chaojin Liu, Yuansheng Wang, Xiaoyan Zhang, Yuqiong Wu, Fangchuan Chen, Synergistic Photothermal and Photodynamic Therapy against Bacterial Infections Using Carbon Quantum Dots Modified Molybdenum Disulfid, *ACS Applied Nano Materials,* **2s025**, 8, 16, 8499-8510.